

Structure of rarefied PbGeO_3 glass: a molecular dynamics study

JAROSŁAW RYBICKI, AGNIESZKA WITKOWSKA, JAROSŁAW BOŚKO

Department of Solid State Physics, Faculty of Technical Physics and Applied Mathematics, Technical University of Gdańsk, ul. Narutowicza 11/12, 80-952 Gdańsk, Poland, and TASK Computer Centre, ul. Narutowicza 11/12, 80-952 Gdańsk, Poland.

GIORGIO MANCINI, SANDRO FELIZIANI

INFN UdR Camerino, Istituto di Matematica e Fisica, Università di Camerino, Via Madonna delle Carceri, Camerino (MC), Italia.

The present contribution is dedicated to a molecular dynamics (MD) study of the structure of rarefied lead-germanate glasses of composition PbGeO_3 . The simulations have been performed in the constant volume regime for systems with densities of 3000, 4000, 5000 and 6285 kg/m^3 , using a two-body potential (Born–Mayer repulsive forces, and Coulomb forces due to full ionic charges). The information on short-range correlations was obtained in a conventional way (from radial and angular distribution functions), while the middle-range order was studied via cation-anion ring analysis. In the paper the short and medium range order in the rarefied glasses is discussed and compared with the structure of the PbGeO_3 glass in normal conditions.

1. Introduction

Lead-silicate and lead-germanate glasses have been extensively investigated because of their numerous practical applications (*e.g.*, [1], [2]). The best known are lead-silicate glasses, $x\text{PbO}(1-x)\text{SiO}_2$, $0 \leq x \leq 0.95$. They have high density, high thermal expansion coefficient, good transparency in the infrared range, and high refraction index (up to 2.15 for high PbO contents), and find wide industrial applications, *e.g.*, in electronics and optoelectronics [2]–[4]. Lead-germanate glasses, $x\text{PbO}(1-x)\text{GeO}_2$, $0 \leq x \leq 0.67$, are investigated to much lesser extent, and until now have found fewer practical applications [5], [6].

The present contribution is dedicated to a molecular dynamics study of the structure of rarefied lead-germanate glass of composition PbGeO_3 . Our numerical experiment was motivated by the fact that homogeneous samples of lead-silicate and lead-germanate glasses produced in different ways can have different densities (up to 20% dispersion around the mean values). In this paper, the molecular dynamics method is used to describe the characteristic structural features of low density states of the PbGeO_3 glass. In Section 2, we describe in

brief the simulation technique applied, and the data analysis methods. The simulation results are described, discussed and compared with the available experimental data in Sec. 3. Section 4 contains conclusions.

2. Simulation technique

Molecular dynamics simulations are at present widely used for structural modelling. The method consists in numerical solution of the classical many-body problem of interacting particles, so that the trajectories of all particles within a simulation box are found. Suitable averaging procedures over atomic trajectories yield the structural and thermodynamical information on the system.

Our MD simulations of lead-germanate glasses were performed in the constant volume regime. The atoms were assumed to interact by a two-body potential (Born–Mayer repulsive forces, and Coulomb forces due to full ionic charges, calculated with the aid of the standard Ewald technique). The potential parameterisation was taken from [7]. The number of atoms within the simulation box was equal to 2500 (500 Pb, 500 Ge and 1500 O atoms). Depending on the system density, the edge of the cubic simulation box varied from about 30 to about 45 Å. The pressures were calculated during the sampling runs from the virial theorem. The systems of densities of 3000, 4000, 5000, 6285 kg/m³ were initiated at the nominal temperature $T = 300$ K using the skew start technique. Then the samples were being equilibrated over 40000 fs time steps. The temperature scaling was being applied whenever the rolling average of the temperature (calculated over 100 time steps) was going out of the interval $(T - \Delta T, T + \Delta T)$, $\Delta T = 30$ K. Equilibrated systems were sampled in 10000 fs time steps.

The structural information on short-range correlations was obtained in a conventional way, *i.e.*, from radial and angular distribution functions. The middle-range order was studied via cation-anion ring analysis, performed using a new highly efficient redundancy aware algorithm [8]–[10].

3. Results and discussion

The peak profile in the RDF, $g(r)$, is given by

$$g(r) = \frac{Np(r)}{4\pi\rho r^2} \quad (1)$$

where N is the co-ordination number, ρ is the density. According to [11], [12], the bond length probability density $p(r)$ is described by a Γ -like distribution. The corresponding formula, for $(r-R)\beta > -2\sigma$, reads

$$p(r) = \frac{2}{\sigma|\beta|\Gamma(4/\beta^2)} \left(\frac{4}{\beta^2} + \frac{2(r-R)}{\sigma\beta} \right)^{\frac{4}{\beta^2}-1} \exp \left[- \left(\frac{4}{\beta^2} + \frac{2(r-R)}{\sigma\beta} \right) \right]. \quad (2)$$

Here, R is the average distance, σ^2 is the variance, β is the asymmetry parameter and $\Gamma(x)$ is the Euler's gamma function calculated for $x = 4/\beta^2$.

3.1. Short-range order — GeO_2 subsystem

Table 1 contains the positions of the maxima R_0 of first RDF peaks, and the corresponding first co-ordination numbers (in parenthesis), simply read at the minimum of the RDF between two first peaks. One can easily note a relative stability of the inter-atomic distances, accompanied by significant variations of the first co-ordination numbers. Several best-fit R , N , σ^2 and β values for chosen densities and RDFs are shown in Tab. 2. The R values, *i.e.*, the average inter-atomic distances, appear to be somewhat greater than the corresponding most probable distances R_0 . Moreover, the density dependence of R is weaker than that of R_0 . The co-ordination numbers N determined from Eqs. (1), (2) are lower than those read at the distance corresponding to the first minimum of the RDFs, since in the former case the contribution of the second peak is automatically eliminated. However, the general tendencies in the density dependence of the inter-atomic distances and co-ordination numbers are similar for both approaches.

Table 1. The positions of the first RDF peak maxima R_0 at various densities ρ for the PbGeO_3 system. The co-ordination numbers, read in the RDF minima between the two first peaks are given in parenthesis.

| ρ [kg/m^3] | Pb-Pb [\AA] | Pb-Ge [\AA] | Pb-O [\AA] | Ge-Ge [\AA] | Ge-O [\AA] | O-O [\AA] |
|----------------------------|------------------------|------------------------|-----------------------|------------------------|-----------------------|----------------------|
| 3000 | 3.86 (3.2) | 3.74 (2.4) | 2.24 (3.2) | 3.36 (2.1) | 1.64 (3.8) | 2.72 (3.9) |
| 4000 | 3.64 (4.0) | 3.66 (2.8) | 2.26 (3.5) | 3.37 (2.3) | 1.66 (3.9) | 2.70 (4.1) |
| 5000 | 3.64 (5.0) | 3.66 (3.2) | 2.28 (3.9) | 3.37 (2.4) | 1.66 (4.0) | 2.68 (4.3) |
| 6285 | 3.50 (5.8) | 3.58 (4.1) | 2.32 (4.4) | 3.36 (2.6) | 1.68 (4.1) | 2.68 (4.5) |

Table 2. The best-fit values of R , N , σ^2 and β parameters for PbGeO_3 glass.

| ρ [kg/m^3] | RDF | R [\AA] | N | σ^2 [\AA] ² | β |
|----------------------------|------|----------------------|------|--|---------|
| 3000 | Ge-O | 1.69 | 3.83 | 0.0089 | 0.51 |
| 3000 | O-O | 2.78 | 3.78 | 0.0331 | 0.65 |
| 6285 | Ge-O | 1.69 | 3.95 | 0.0048 | 0.58 |
| 6285 | O-O | 2.73 | 4.19 | 0.0220 | 0.50 |

Figure 1 shows the first peaks of radial distribution functions related to Ge^{4+} cations for two densities. The corresponding angular distribution functions are shown in Fig. 2. It can be seen from Fig. 1 that the first RDF peaks reveal rather significant asymmetry (note high values of the parameter β in Tab. 2). With decreasing density the most probable Ge-O distance becomes shorter than in normal conditions (*i.e.*, at the density of 6285 kg/m^3), and the average oxygen co-ordination number around Ge decreases from about 4.1 to 3.8. The average O-O distance slightly increases with decreasing density. With increasing density the fraction of germanium atoms co-ordinated with four oxygen atoms increases (from about 80% at 3000 kg/m^3 to about 97% at 6285 kg/m^3). Using the data on inter-atomic distances listed in Tab. 1 and inter-bond angle distributions from Fig. 2, one concludes that the basic structural units related to Ge^{4+} cations are

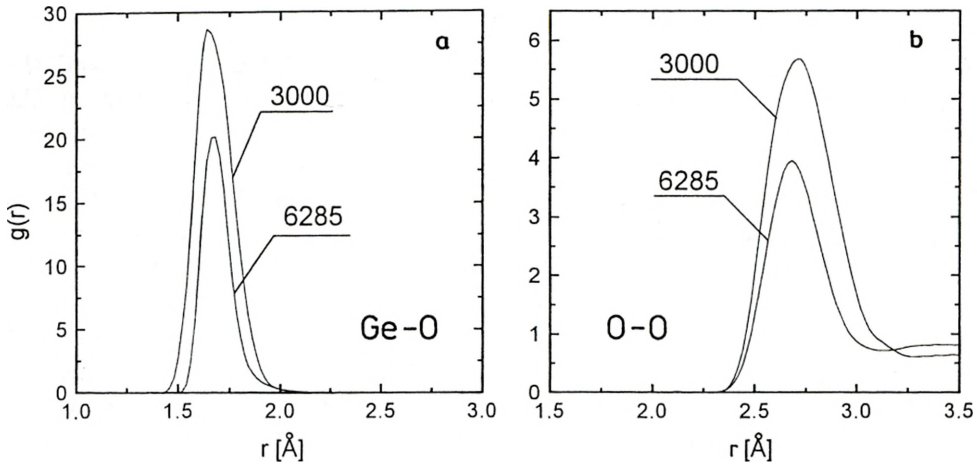


Fig. 1. Radial distribution functions related to the glass forming Ge^{4+} cation in PbGeO_3 glass. The values in the figures indicate the system densities in kg/m^3 ; Ge-O correlation (a), O-O correlation (b).

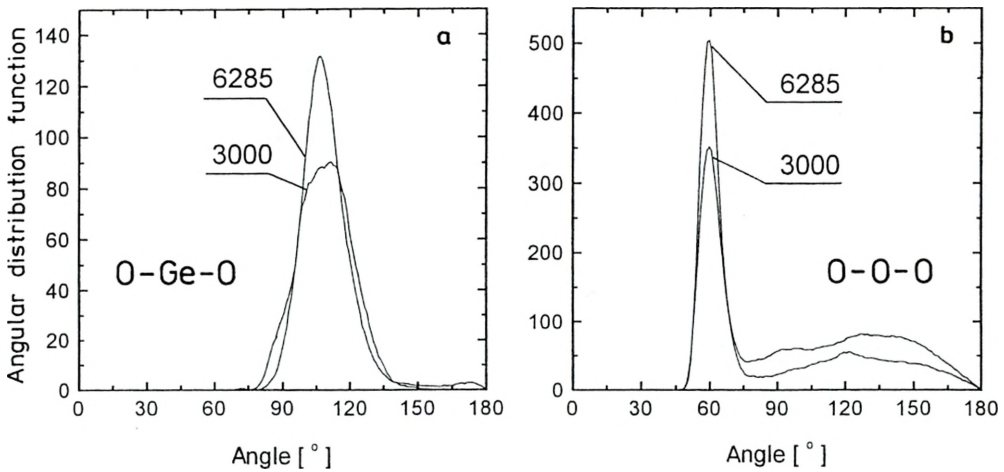


Fig. 2. Angular distribution functions in PbGeO_3 glasses of various densities (in kg/m^3); O-Ge-O correlation (a), O-O-O correlation (b).

GeO_4 tetrahedra. They are the dominant structural units in the whole density range we have considered (3000–6285 kg/m^3). Let us introduce the tetrahedrality parameter T [13]

$$T = \frac{\sum_{i,j} (l_i - l_j)^2}{l^2} \quad (3)$$

where l_i is the length of the i -th tetrahedron edge, and l is the average tetrahedra edge. The distribution of the values of the tetrahedrality parameter T practically does not depend on the glass density. The values T are lower than 0.04 for 90–95% of

all GeO₄ units. At low densities some GeO₃ triangular, rather flat groups appear, whereas at higher densities small fractions of GeO₅ (2%) and GeO₆ (1%) are detected. Thus, our simulations give no evidence of germanium anomaly (appearance of GeO₆ groups in the presence of other oxides in GeO₂). This result is compatible with recent experimental data provided by X-ray scattering analysis [14]. It is worth noting that our simulation data predict quite marginal density dependence the Ge–Ge distance, accompanied by a change of the Ge–Ge co-ordination number (an increase from 2.1 at 3000 kg/m³ to 2.6 at 6285 kg/m³).

3.2. Short-range order – PbO subsystem

In the density range considered both the Pb–O distance and the average oxygen co-ordination number decreases with decreasing density (see Tab. 1). The fraction of lead atoms co-ordinated with four oxygen atoms increases with density, but does not exceed 50%. The PbO₄ groups can be classified as tetrahedra or square pyramids. Tetrahedral structures are dominant for all the densities and the contribution of tetrahedra increases with density (from about 60% at 3000 kg/m³ to about 80% at 6285 kg/m³). The values of the tetrahedrality parameter T are higher for lower densities than for higher densities, *i.e.*, at lower densities the tetrahedral PbO₄ groups are more distorted. At 3000 kg/m³ and 6285 kg/m³ the parameter T is lower than 0.2 for about 60% and 85% of all PbO₄ tetrahedra detected. For the square-pyramid PbO₄ groups we defined the following shape estimator

$$P = \frac{\sum_{i,j} (l_{\text{Pb-O},i} - l_{\text{Pb-O},j})^2}{l_{\text{Pb-O}}^2} + \frac{\sum_{i,j} (l_{\text{O-O},i} - l_{\text{O-O},j})^2}{l_{\text{O-O}}^2} \quad (4)$$

where $l_{\text{Pb-O},i}$ is the length of the i -th Pb–O edge, and $l_{\text{Pb-O}}$ is the average length of the Pb–O edges, and similarly, $l_{\text{O-O},i}$ is the length of the i -th O–O edge, and $l_{\text{O-O}}$ is the average length of the O–O edges. The distribution of values P for pyramid-like PbO₄ groups remains almost independent of density, and over 60% of the structures are characterised by $P \leq 0.2$.

3.3. Medium-range order – Ge–O–Ge–O– ... and Pb–O–Pb–O– ... rings

As far as the short-range order is concerned, the inspection of the radial and angular distribution functions is sufficient for a quite detailed description of the first co-ordination shells of atoms. However, in order to describe the second and further co-ordination shells, *i.e.*, to describe the middle range order, one should use more advanced methods of the structural analysis, such as ring analysis [8]–[10]. A closed chain of chemically bonded atoms, consisting of N cations and N anions will be called an N -member ring or a ring of length N . In what follows we discuss the length statistics of linearly independent (basal) rings that span the full graph representing chemically bonded atoms. The graphs were constructed according to a simple adjacency criterion, with cut-off radii equal to 2.1 Å, and 3.0 Å for Ge–O and Pb–O distances, respectively.

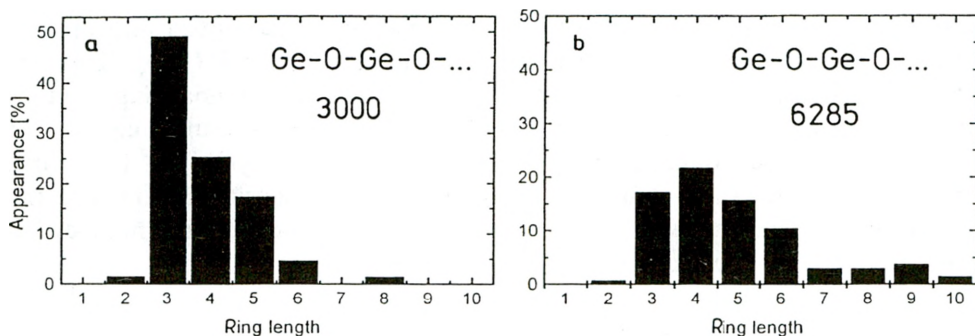


Fig. 3. Distributions of lengths of Ge-O-Ge-O-... rings for densities of 3000 kg/m³ (a) and 6285 kg/m³ (b).

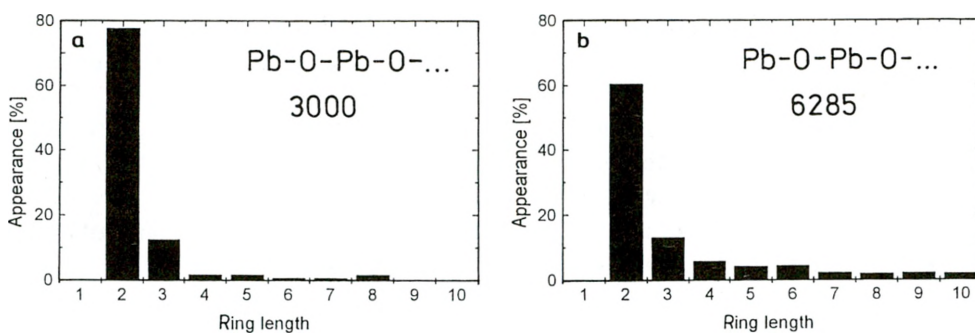
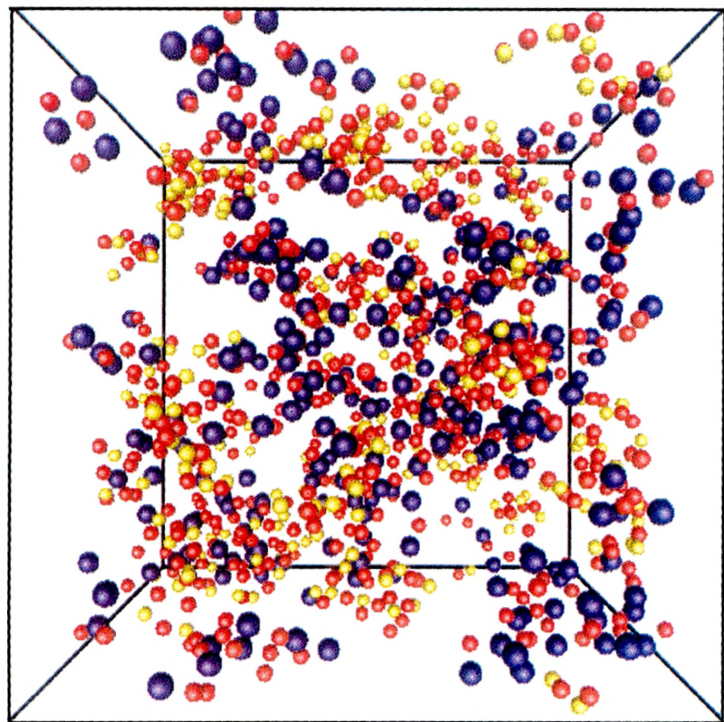


Fig. 4. Distributions of lengths of Pb-O-Pb-O-... rings for densities of 3000 kg/m³ (a) and 6285 kg/m³ (b).

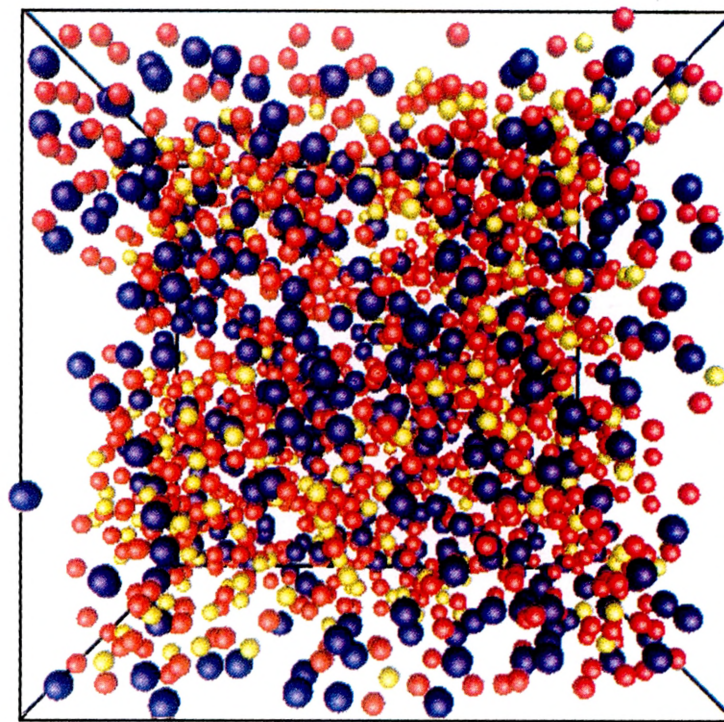
Figure 3 shows the length distribution of the Ge-O-Ge-O-... rings for two densities. As one can see, in low-density phases the fraction of 2-member rings, corresponding to edge sharing GeO₄ tetrahedra, is marginal, similarly as in the normal density state. However, the fraction of 3-member rings significantly increases on decreasing density. Simultaneously, at low densities practically no long (say, longer than 6) rings are present (at the normal density single rings of length up to 30 were detected).

Figure 4 shows the length distribution of the Pb-O-Pb-O-... rings at low and normal density. With decreasing density the lead-oxygen basal rings become systematically shorter, and the contribution of 2-member rings, corresponding to edge sharing structural units increases.

Such an evolution of the cation-anion ring lengths suggests that at low densities the structural units related to germanium and lead cations tend to create compact groups containing three corner-sharing GeO₄ units (forming strained 3-member Ge-O rings), and two edge-sharing PbO₄ or PbO₅ units (forming 2-member Pb-O rings). The compact clusters of lead and germanium units are interconnected by GeO₄-Pb-GeO₄-Pb-GeO₄-... chains. The glass structure at normal density is much more uniform (see Fig. 5).



300 kg/m³



6285 kg/m³

Fig. 5. Snapshots of atom configurations in the last simulation steps for the densities of 3000 kg/m³ and 6285 kg/m³. Only the atoms belonging to the basal Ge–O–Ge–O–... and Pb–O–Pb–O–... rings are shown. Blue balls – Pb atoms, yellow balls – Ge atoms, red balls – O atoms. The radii of balls in both figures are equal – the optical difference results from different box sizes, which are obviously calculated from the structure density.

4. Conclusions

We have presented the results of preliminary MD simulations of the PbGeO_3 glasses of various density. In order to make the low-density effects more pronounced we performed simulations starting from extremely low density of 3000 kg/m^3 . The MD data suggest the following conclusions:

1. The short range ordering changes rather slightly in the density range $3000 - 6285 \text{ kg/m}^3$. Regular GeO_4 units dominate in the GeO_2 subsystem for all the densities. No germanium anomaly is reported. The PbO subsystem has a much more complex structure. Both PbO_4 tetrahedra and PbO_4 square pyramids were detected. The tetrahedra are more regular and more frequent at higher densities.

2. The medium range order undergoes radical changes: on decreasing density the number of short, strained rings significantly increases, and long rings disappear. At extremely low densities the structure seems to become non-homogeneous.

Acknowledgments – The opportunity to perform our simulations at the TASK Computer Centre in Gdańsk, Poland, is kindly acknowledged.

References

- [1] RULLER J.A., SHELBY J.E., *Phys. Chem. Glass.* **33** (1992), 177.
- [2] DUMBAUGH W., LAPP J.C., *J. Am. Ceram. Soc.* **75** (1992), 2315.
- [3] YAMADA K., MATSUMOTO A., NIIMURA N., *et al.*, *J. Phys. Soc. Jpn.* **55** (1986), 831.
- [4] CORMIER G., PERES T., CAPOBIANCO J.A., *J. Non-Cryst. Solids* **195** (1996), 125.
- [5] FELTZ A., *Amorphous Inorganic Materials and Glasses*, VCH, Weinheim 1993.
- [6] LEZAL D., PEDLIKOVA J., HOVAK J., *J. Non-Cryst. Solids* **196** (1996), 178.
- [7] RYBICKA A., *The structure and properties of lead-silicate and lead-germanate glasses: a molecular dynamics study* (in Polish), PhD Thesis, Technical University of Gdańsk, Gdańsk, Poland, 1999.
- [8] MANCINI G., *TASK Quart.* **1** (1997), 89.
- [9] MANCINI G., *Comp. Phys. Commun.* (submitted).
- [10] BERGMAŃSKI G., RYBICKI J., MANCINI G., *TASK Quart.* **4** (2000), 555.
- [11] D'ANGELO P., DI NOLA A., FILIPPONI A., *et al.*, *J. Chem. Phys.* **100** (1994), 985.
- [12] FILIPPONI A., DI CICCIO A., *Phys. Rev. B* **51** (1995), 12322.
- [13] BROSTOW W., CHYBICKI M., LASKOWSKI R., *et al.*, *Phys. Rev. B* **57** (1998), 13448.
- [14] CERVINKA L., *J. Non-Cryst. Solids* **276** (2000), 19.

Received September 18, 2000